

The TspanC8 Subgroup of Tetraspanins Interacts with A Disintegrin and Metalloprotease 10 (ADAM10) and Regulates Its Maturation and Cell Surface Expression^{*[5]}

Received for publication, February 24, 2012, and in revised form, September 30, 2012. Published, JBC Papers in Press, October 3, 2012, DOI 10.1074/jbc.M112.416503

Elizabeth J. Haining[‡], Jing Yang[‡], Rebecca L. Bailey[‡], Kabir Khan[‡], Richard Collier[‡], Schickwann Tsai[§], Steve P. Watson[¶], Jon Frampton^{||}, Paloma Garcia^{||}, and Michael G. Tomlinson^{‡1}

From the [‡]School of Biosciences, College of Life and Environmental Sciences and Schools of [¶]Clinical and Experimental Medicine and ^{||}Immunity and Infection, College of Medical and Dental Sciences, University of Birmingham, Birmingham B15 2TT, United Kingdom and [§]Division of Hematology, Department of Medicine, University of Utah, Salt Lake City, Utah 84132

Background: ADAM10 is a transmembrane metalloprotease that regulates development, inflammation, cancer, and Alzheimer disease.

Results: The TspanC8 subgroup of tetraspanin membrane proteins interacts with and promotes ADAM10 maturation and cell surface localization.

Conclusion: This study defines the TspanC8 tetraspanins as essential regulators of ADAM10.

Significance: Focusing on specific TspanC8-ADAM10 complexes may allow ADAM10 therapeutic targeting in a cell type- and/or substrate-specific manner.

A disintegrin and metalloprotease 10 (ADAM10) is a ubiquitous transmembrane metalloprotease that cleaves the extracellular regions from over 40 different transmembrane target proteins, including Notch and amyloid precursor protein. ADAM10 is essential for embryonic development and is also important in inflammation, cancer, and Alzheimer disease. However, ADAM10 regulation remains poorly understood. ADAM10 is compartmentalized into membrane microdomains formed by tetraspanins, which are a superfamily of 33 transmembrane proteins in humans that regulate clustering and trafficking of certain other transmembrane “partner” proteins. This is achieved by specific tetraspanin-partner interactions, but it is not clear which tetraspanins specifically interact with ADAM10. The aims of this study were to identify which tetraspanins interact with ADAM10 and how they regulate this metalloprotease. Co-immunoprecipitation identified specific ADAM10 interactions with Tspan5, Tspan10, Tspan14, Tspan15, Tspan17, and Tspan33/Penumbra. These are members of the largely unstudied TspanC8 subgroup of tetraspanins, all six of which promoted ADAM10 maturation. Different cell types express distinct repertoires of TspanC8 tetraspanins. Human umbilical vein endothelial cells express relatively high levels of Tspan14, the knockdown of which reduced ADAM10 surface expression and activity. Mouse erythrocytes express predominantly Tspan33, and ADAM10 expression was substantially reduced in the absence of this tetraspanin. In contrast, ADAM10 expression was normal on Tspan33-deficient mouse platelets in which Tspan14 is the major TspanC8 tetraspanin. These results define

TspanC8 tetraspanins as essential regulators of ADAM10 maturation and trafficking to the cell surface. This finding has therapeutic implications because focusing on specific TspanC8-ADAM10 complexes may allow cell type- and/or substrate-specific ADAM10 targeting.

The proteolytic cleavage, or “shedding,” of the extracellular regions (ectodomains) of transmembrane proteins is emerging as an important mechanism for the regulation of cell development and function (1–3). A disintegrin and metalloprotease 10 (ADAM10)² is a type 1 transmembrane protein that is ubiquitously expressed and functions as an ectodomain sheddase for over 40 transmembrane target proteins (4). ADAM10-deficient mice die at embryonic day 9.5, consistent with the essential role of ADAM10 in the cleavage and activation of Notch, which is central to most cell fate decision-making processes during metazoan development (5). Amyloid precursor protein is an ADAM10 target that is central to Alzheimer disease (6). Cleavage of amyloid precursor protein by β - and γ -secretases gives rise to the pathogenic amyloid β -peptide that forms the amyloid plaques in the brains of Alzheimer disease patients. Counteracting this is the α -secretase activity of ADAM10 that cleaves amyloid precursor protein at a third site, thus preventing release of the pathogenic peptide. Indeed, transgenic overexpression of ADAM10 prevents amyloid plaque deposition in a mouse model of Alzheimer disease, suggesting that ADAM10 is a promising target for disease treatment in humans (6). ADAM10 targets in the vasculature include the platelet-activating collagen receptor glycoprotein VI (7, 8) and endothelial proteins with roles in angiogenesis and inflammation, such as vascular endothelial growth factor receptor 2 (9), the junctional

* This work was supported by two Biotechnology and Biological Sciences Research Council studentships (to E. J. H. and R. L. B.), a British Heart Foundation (BHF) chair (to S. P. W.), a Science City Research Alliance fellowship (to P. G.), and BHF Senior Research Fellowship FS/08/062/25797 (to M. G. T.).

[5] This article contains supplemental Figs. I–IV.

¹ To whom correspondence should be addressed. Tel.: 44-121-414-2507; Fax: 44-121-414-5925; E-mail: m.g.tomlinson@bham.ac.uk.

² The abbreviations used are: ADAM10, a disintegrin and metalloprotease 10; VE, vascular endothelial; Fc γ RIIa, Fc γ receptor IIa; DTSSP, 3,3'-dithiobis(sulfosuccinimidyl)propionate; ER, endoplasmic reticulum; Tspan, tetraspanin.

TspanC8 Subgroup Regulates ADAM10 Maturation and Expression

adhesion molecule VE-cadherin (10), and transmembrane chemokines CX3CL1 and CXCL16 (11). Despite the importance of ADAM10, the regulation of its trafficking, activation, and localization to targets is poorly understood. Mechanistic characterization of these events is essential if we are to harness the potential of ADAM10 as a therapeutic target.

The regulation of transmembrane proteins by their compartmentalization into membrane microdomains is a concept that has developed over recent years through the study of neuronal and immunological synapses, lipid rafts, caveolae, and tetraspanins. The latter are a superfamily of four-transmembrane proteins that number 33 in humans (12, 13). Tetraspanins possess two extracellular regions, the larger of which has four to eight conserved cysteine residues that form structurally important disulfide bonds. They appear to fold into compact rod-shaped structures that only project about 5 nm from the plasma membrane and play a fundamental organizing role by self-associating to form microdomains. Specific tetraspanins recruit so-called “partner” proteins into the microdomains. These partners include certain integrins, immunoglobulin superfamily proteins, and proteases, and in some cases, their interaction with tetraspanins is essential for normal biosynthesis and trafficking to the plasma membrane (12, 13). Tetraspanin microdomains can also facilitate cell adhesion and signaling by providing platforms in which associated proteins can be clustered. For example, the endothelial cell adhesion molecules ICAM-1, VCAM-1, and P-selectin require clustering by tetraspanins CD9, CD151, and CD63, respectively, for efficient capture of leukocytes from the circulation (14, 15). In addition, Frizzled-4 appears to require clustering by tetraspanin Tspan12 to allow appropriate β -catenin signaling for development of the retinal vasculature in mice and humans (16–18). In contrast, vascular development in mice is normal in the absence of CD151, but pathological angiogenesis is defective, possibly due to the well characterized regulation of laminin-binding integrins $\alpha 3\beta 1$ and $\alpha 6\beta 1$ by this tetraspanin (19). On platelets, CD151 and Tspan32 are essential for thrombus formation *in vivo* (20, 21), and Tspan33 (previously named Penumbra) is required for normal erythropoiesis (22), although the mechanisms responsible for these phenotypes remain unclear.

ADAM10 was recently shown to predominantly localize to tetraspanin microdomains in human leukocyte cell lines (23). In addition, tetraspanin antibodies could promote ADAM10 activity as measured by shedding of two ADAM10 targets, TNF- α and EGF (23). A second study showed that ADAM10 co-immunoprecipitated with Tspan12 in human breast cancer and neuroblastoma cell lines (24). Tspan12 also promoted ADAM10 maturation, which involves the cleavage of its prodomain by proprotein convertases during trafficking to the plasma membrane. Moreover, ADAM10 activity was enhanced by Tspan12 as detected by shedding of the ADAM10 target amyloid precursor protein (24). However, Tspan12 is unlikely to be the only tetraspanin that regulates ADAM10 because it does not share the ubiquitous expression profile of the metalloprotease, instead appearing relatively restricted to endothelial cells of the retina, meninges of the brain, and smooth muscle cells of the colon (16). Indeed, Tspan12 does not appear to be expressed by the platelet (25–29), a cell type on which we chose

to initially focus because it expresses many other tetraspanins as well as ADAM10. Therefore, in the present study, we tested the hypothesis that one or more platelet tetraspanins could interact with and regulate ADAM10. This led to the identification of a subgroup of six related, but largely unstudied, tetraspanins that fulfilled these criteria that we termed the TspanC8 tetraspanins due to the eight cysteine residues within their main extracellular region. These tetraspanins appear to play a common role in promoting ADAM10 maturation and trafficking to the plasma membrane.

EXPERIMENTAL PROCEDURES

Antibodies—Mouse anti-human mAbs were 11G2 (23) and 163003 (R&D Systems) to ADAM10, 11B1 to CD151 (30), IV.3 to Fc γ RIIa (Medarex), and 1.3 to PECAM-1 (a gift from Peter Newman, Wisconsin, MI). The rat anti-mouse ADAM10 mAb was 139712 (R&D Systems), control mouse IgG1 was MOPC-21 (Sigma), and control rat IgG2A was 54447 (R&D Systems). Polyclonal antibodies were the AB936 goat anti-human ADAM10 (R&D Systems) and sc-6458 goat anti-VE-cadherin C terminus (Santa Cruz Biotechnology). Anti-epitope tag antibodies were mouse anti-FLAG mAb M2 and rabbit anti-FLAG (Sigma), rabbit anti-HA mAb C29F4 (Cell Signaling Technology), and mouse anti-GFP mAb 3E1 (Cancer Research UK).

Expression Constructs—Tetraspanin expression constructs with N-terminal FLAG tags were generated by cloning tetraspanin cDNAs into the pEF6-FLAG vector (27), which is a modified version of pEF6/*Myc*-His A (Invitrogen). Tetraspanin constructs with N-terminal GFP tags were similarly made using the pGFP-C vector (BioSignal Packard). Tetraspanin cDNAs were generated by PCR from cDNA derived from the HEK293T cell line, primary mouse megakaryocytes, or megakaryocyte-like cell line L8057. Palmitoylation mutants of human tetraspanins were generated by a two-PCR strategy (31) that mutated all cysteine residues at the membrane-cytoplasm interface to serines. These were amino acids 13, 80, 89, and 95 for Tspan14; 12, 101, 287, 288, and 290 for Tspan15; and 81, 83, 92, and 100 for Tspan33. The HA-tagged bovine ADAM10 in the pcDNA3 vector has been described previously (32).

Mice—Tspan33/Penumbra knock-out mice have been described previously (22). All animal maintenance and experiments had appropriate Home Office approval and licensing according to Animals (Scientific Procedures) Act 1986. Knock-out mice and littermate controls were generated by breeding heterozygote animals. All animals used for experiments were aged 8 weeks or older.

Cell Culture and Transfection—All cell culture reagents were from PAA unless stated. The human embryonic kidney (HEK)-293T (HEK-293 cells expressing the large T-antigen of simian virus 40) cell line was cultured in Dulbecco's modified Eagle's medium (DMEM) containing 10% fetal bovine serum, 4 mM glutamine, 100 units/ml penicillin, and 100 μ g/ml streptomycin. Transfection of HEK-293T cells was carried out using polyethylenimine (Sigma) as described (33). The A549 human lung epithelial cell line was cultured in the same medium as HEK-293T cells. Primary human umbilical vein endothelial cells (HUVECs) were provided by Phil Stone and Gerard Nash (Uni-

versity of Birmingham) from umbilical cords that were obtained with consent from the Birmingham Women's Health Care National Health Service Trust after delivery. HUVECs were maintained in M199 medium supplemented with 10% fetal bovine serum, 4 mM glutamine, 90 μ g/ml heparin (Sigma), and bovine brain extract (34) and used between passages 3 and 6 for all experiments. For siRNA knockdown experiments, A549 and HUVECs were transfected using RNAiMAX transfection reagent and 10 nM Silencer Select siRNA duplexes (Invitrogen).

Purification of Platelets and Megakaryocytes—Washed human platelets were prepared as described previously from whole blood (35). Consent was obtained from each blood donor, and platelet preparation was carried out in agreement with the Declaration of Helsinki (2000) of the World Medical Association and approved by the Ethics Committee at the University of Birmingham. Primary mouse megakaryocytes were isolated using a modified version of the method described previously (36). Bone marrow was flushed under sterile conditions from both femora and tibiae. Harvested cells were treated with ACK red blood cell lysis buffer (0.15 M NH_4Cl , 1 mM KHCO_3 , 0.1 mM Na_2EDTA , pH 7.3) for 5 min at room temperature and then filtered through a 70- μ m nylon mesh filter. To remove non-megakaryocyte lineage cells, they were incubated on ice for 30 min with rat anti-mouse mAbs to Gr-1, CD11b, B220, and CD16/32 (eBioscience) and then depleted using anti-rat magnetic beads (Dyna). The remaining cells were cultured in complete Stempro 34 medium (Invitrogen) supplemented with 20 ng/ml stem cell factor (PeproTech) for 48 h. Non-adherent cells were transferred into fresh complete Stempro 34 medium and supplemented with 20 ng/ml stem cell factor and 50 ng/ml murine thrombopoietin (PeproTech). After a further 3–4 days in culture, the differentiated cells were separated over a 1.5–3% BSA gradient for 45 min, and the mature megakaryocytes were collected from the bottom gradient fraction (36).

Purification of Proerythroblasts—Proerythroblasts were purified from adult mouse bone marrow or fetal liver. For each experiment that used proerythroblasts from adult mice, bone marrow was flushed from both femora and tibiae of three mice. Cells were centrifuged at $300 \times g$ for 5 min at 4 °C, and the pellet was resuspended in ice-cold 5–10% FBS in PBS. Fc receptors were blocked with anti-CD16/32 (eBioscience) for 5 min followed by staining with allophycocyanin-conjugated anti-Ter119 and phycoerythrin-conjugated anti-CD71 (eBioscience) for 60 min on ice in the dark. Ter119 and CD71 double positive erythroblasts were collected using a Beckman Coulter MoFlo high speed cell sorter. For preparation of proerythroblasts from fetal liver, single cell suspensions of fetal liver cells from E12.5 mouse embryos were cultured as described (37). In brief, prepared cells were cultured in Stempro 34 complete medium supplemented with 100 ng/ml murine stem cell factor (PeproTech), 2 units/ml human erythropoietin (Roche Applied Science), and 1 μ M dexamethasone (Sigma) for 7 days. These cfu erythroid-enriched cultures were purified using a Ficoll gradient and cultured in the described medium for a further 2 days at which point the cells were processed for MoFlo flow cytometry sorting as described above.

Cell Surface Biotinylation Experiments—The human platelet cell surface biotinylation experiments were conducted as described (27). For mouse erythrocyte surface biotinylation experiments, whole blood obtained by exsanguinations (35) was centrifuged at $200 \times g$ for 5 min, and the erythrocytes were separated from the platelet-rich plasma layer. Erythrocytes were washed with modified Tyrode's buffer containing 5% acid citrate dextrose (35). The cells were biotinylated with 2 mM EZ-Link sulfo-*N*-hydroxysuccinimide long chain biotin (Thermo Scientific) for 30 min and quenched with 0.1 M glycine. Subsequent cell lysis, immunoprecipitations, and Western blotting were as described (27). For ADAM10 stability studies, A549 cells were transfected with siRNAs and 3 days later were biotinylated with 1 mM EZ-Link sulfo-NHS-LC-biotin (Thermo Scientific) for 30 min and quenched with 0.1 M glycine. Some cells were harvested and frozen immediately, whereas others were returned to culture and harvested and frozen at 24, 36, or 48 h postbiotinylation. Cell pellets were lysed in 1% Triton X-100 lysis buffer (27) containing a protease inhibitor mixture (Sigma). Following centrifugation to remove nuclei and insoluble debris, lysates were subjected to mouse anti-ADAM10 or control MOPC-21 immunoprecipitation for 90 min. The immunoprecipitates were washed with 1% Triton X-100 lysis buffer, separated by SDS-PAGE on non-reducing gels, and Western blotted with IRDye fluorescent neutravidin (LI-COR Biosciences). The results were imaged and quantified on the Odyssey Infrared Imaging System (LI-COR Biosciences).

Cell Surface Chemical Cross-linking Experiments—Two days following transfection with HA-ADAM10 and FLAG-tetraspans, HEK-293T cells were washed with PBS and treated with a 2 mM concentration of the cell surface cross-linker 3,3'-dithiobis(sulfosuccinimidylpropionate) (DTSSP) from Thermo Fisher Scientific for 30 min on ice. The cross-linking was quenched with 0.1 M glycine, and the cells were scraped off and lysed in 1% Triton X-100 lysis buffer (27) containing a protease inhibitor mixture (Sigma). Following centrifugation to remove nuclei and insoluble debris, lysates were supplemented with 0.1% SDS to increase lysis buffer stringency, and mouse anti-FLAG immunoprecipitations were performed overnight using protein G-Sepharose beads (Invitrogen), or anti-GFP immunoprecipitations were performed overnight using GFP-Trap[®] beads (ChromoTek). The immunoprecipitates were washed with 1% Triton X-100, 0.1% SDS lysis buffer and separated by SDS-PAGE on reducing gels to break the disulfide bond within DTSSP, thus allowing co-immunoprecipitated proteins to run at their predicted molecular weights. Western blotting was carried out with anti-HA and anti-FLAG or anti-GFP primary antibodies and specific IRDye fluorescent secondary antibodies (LI-COR Biosciences). The results were imaged and quantified on the Odyssey Infrared Imaging System (LI-COR Biosciences).

Digitonin Lysis Experiments—These were done in a manner similar to the experiments in the previous section except that cells were not subjected to DTSSP cross-linking but were instead directly lysed in 1% digitonin (Merck Millipore) lysis buffer (38) containing a protease inhibitor mixture (Sigma). Immunoprecipitations were done for 90 min rather than overnight and were washed in 1% digitonin lysis buffer.

TspanC8 Subgroup Regulates ADAM10 Maturation and Expression

VE-cadherin Cleavage Assay—This assay was performed as described (10) using HUVECs 3 days post-siRNA transfection. The γ -secretase inhibitor *N*-[*N*-(3,5-difluorophenacetyl)-*L*-alanine]-*S*-phenylglycine *t*-butyl ester (Sigma) at 10 μ M was added 18 h before harvesting the cells to prevent further proteolysis of VE-cadherin after ADAM10 cleavage. The results were imaged and quantified on the Odyssey Infrared Imaging System (LI-COR Biosciences).

Flow Cytometry—For ADAM10 flow cytometry analyses of mouse platelets and erythrocytes, whole blood was obtained by exsanguinations (35), and 5- μ l volumes were stained in 50 μ l of PBS, 1 mM EGTA with 10 μ g/ml FITC-conjugated rat anti-mouse ADAM10 mAb or negative control FITC-conjugated rat IgG2A. Platelets and erythrocytes were analyzed using a FACSCalibur (BD Biosciences) by first gating the cells according to size. The level of ADAM10 expression on each cell type was then calculated by subtracting the negative control geometric mean fluorescence intensity from the specific ADAM10 value. ADAM10 flow cytometry analyses of HUVECs were performed by first scraping off the cells and then staining 1×10^5 cells with 10 μ g/ml FITC-conjugated mouse anti-human ADAM10 mAb or negative control FITC-conjugated mouse IgG1. Following FACSCalibur analysis, the level of ADAM10 expression was calculated as described above.

Quantitative PCR—RNA was isolated using the Norgen Biotek Total RNA Purification kit and used to make cDNA using the Invitrogen High Capacity cDNA Reverse Transcriptase kit. Quantitative PCRs used a TaqMan 2 \times Enzyme Master Mix, TaqMan probes, and custom primers from Invitrogen. Following 44 cycles in an ABI Prism[®] 7000 Sequence Detection System (Applied Biosystems), cycle threshold (Ct) values were converted to Δ Ct by subtracting Ct values for the glyceraldehyde-3-phosphate dehydrogenase (GAPDH) housekeeping gene, and then Δ Ct values were adjusted such that the highest wild-type value averaged to 100.

Bioinformatics and Statistical Analyses—Multiple sequence alignment of protein sequences of the 33 human tetraspanins was conducted using Clustal Omega (39). Statistical analyses were carried out using a one-way analysis of variance followed by Dunnett's test.

RESULTS

ADAM10 Associates with Tetraspanins in Platelets—The ectodomain sheddase ADAM10 has been reported to associate with tetraspanins in a variety of cell lines (23, 24). The platelet was initially selected as a good model for a human cell line that expresses ADAM10 and multiple tetraspanins. Thus, to determine whether ADAM10 interacts with tetraspanins on human platelets, they were surface-biotinylated and subjected to lysis in two different detergents: 1% Brij97, which largely retains tetraspanin-tetraspanin interactions, and the more stringent 1% Triton X-100, which disrupts tetraspanin-tetraspanin interactions (12). Following immunoprecipitation of ADAM10 or control proteins, co-immunoprecipitated surface proteins were detected by streptavidin Western blotting. Under Brij97 lysis, ADAM10 was found to co-immunoprecipitate a pattern of proteins strikingly similar to CD151 (Fig. 1), which was chosen because it is the best characterized platelet tetraspanin (21).

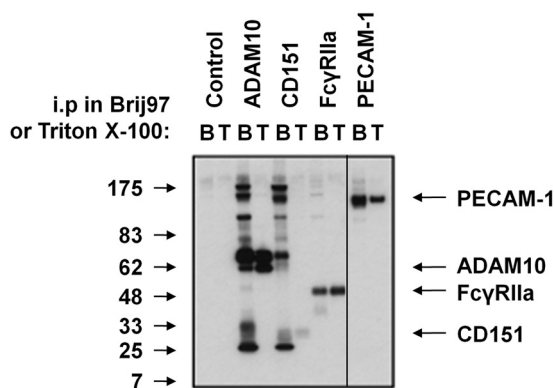


FIGURE 1. ADAM10 is a component of tetraspanin microdomains on platelets because ADAM10 immunoprecipitates from platelet lysates contain a characteristic pattern of tetraspanins and associated proteins. Human platelets were surface-biotinylated and lysed in 1% Brij97 lysis buffer (labeled B), which largely maintains tetraspanin-tetraspanin interactions and hence microdomain integrity, or in 1% Triton X-100 (labeled T), which disrupts tetraspanin microdomains (12). Lysates were immunoprecipitated (*i.p.*) with negative control IgG or mAbs to ADAM10, tetraspanin CD151 (positive control), Fc γ RIIa, or PECAM-1 (non-tetraspanin-associated negative control). Immunoprecipitates were analyzed by streptavidin Western blotting to detect biotinylated proteins. The separating line between the Fc γ RIIa and PECAM-1 data indicates that the latter was from a different part of the same gel.

This pattern of ADAM10- and CD151-associated proteins was lost in more stringent Triton X-100 lysis buffer (Fig. 1), suggesting that the observed bands represent the main components of tetraspanin microdomains. In contrast to ADAM10 and CD151, immunoprecipitations of Fc γ RIIa and PECAM-1 yielded the proteins themselves but no major associated proteins (Fig. 1). These were chosen as controls because they are not known to associate with tetraspanins but have expression levels comparable to that of ADAM10 (Fig. 1). These data suggest that ADAM10 is a component of platelet tetraspanin microdomains but provide no evidence for a direct ADAM10-CD151 interaction. Indeed, such a direct interaction would appear unlikely because it was not retained in Triton X-100 lysis buffer. Instead, one or more other platelet tetraspanins may directly interact with ADAM10 and act to bridge indirect ADAM10-CD151 interactions.

The Platelet Tetraspanins Tspan14, Tspan15, and Tspan33 Interact with and Promote ADAM10 Maturation—Tspan12 was reported to interact more strongly with ADAM10 than other tetraspanins that were tested (CD9, CD81, CD82, and CD151) and to promote ADAM10 maturation (24). However, Tspan12 is not as ubiquitously expressed as ADAM10 (16), suggesting that ADAM10 might be regulated by additional tetraspanins. Indeed, an extensive proteomics analysis of the human platelet cell surface did not detect Tspan12 but did identify at least 10 other tetraspanins (26, 29). In addition, recent platelet transcriptomics profiling (28) found mRNA for 22 and 21 tetraspanins in human and mouse, respectively, but Tspan12 was not among the human tetraspanins and was only very weakly detected in mouse (supplemental Fig. 1).

To determine whether one or more platelet tetraspanins could interact with ADAM10, a panel of 10 was selected based on their identification on human platelets by proteomics (26, 29). Because antibodies are not available to most of these tetraspanins, a co-transfection system in HEK293T cells was

TspanC8 Subgroup Regulates ADAM10 Maturation and Expression

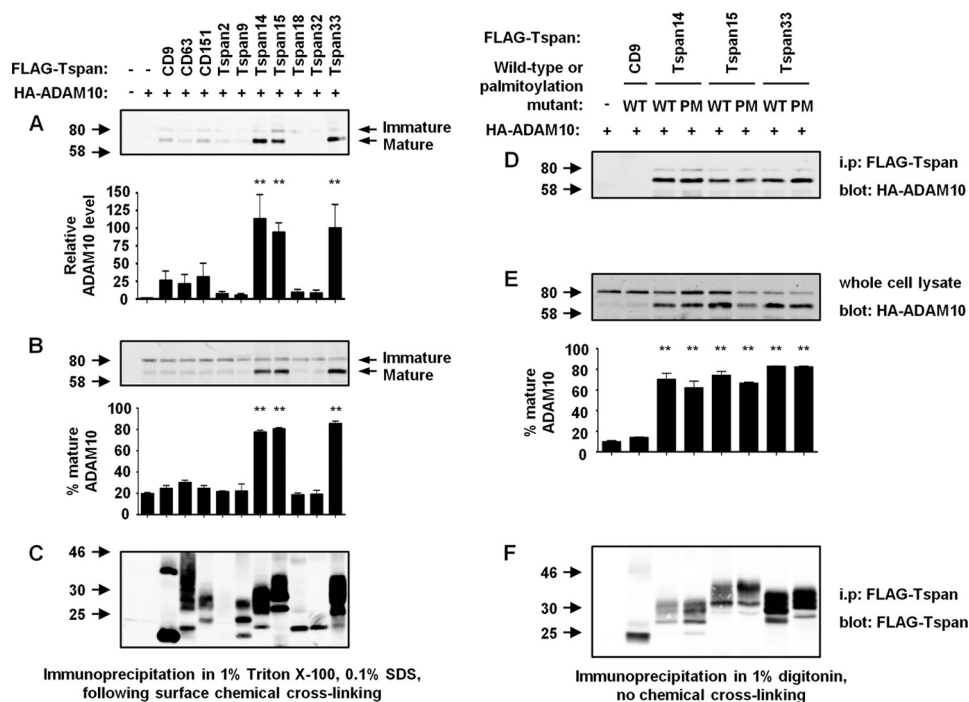


FIGURE 2. Tspan14, Tspan15, and Tspan33 interact with and promote the maturation of ADAM10. A–C, HEK-293T cells were transfected with FLAG-tagged mouse forms of a panel of 10 tetraspanins previously found to be expressed by human platelets (26, 29) in the absence (–) or presence (+) of HA-tagged bovine ADAM10. The cells were surface-cross-linked with DTSSP, lysed in 1% Triton X-100, and subjected to anti-FLAG immunoprecipitation (*i.p.*) in 1% Triton X-100 containing 0.1% SDS. A, the immunoprecipitates were reduced to break the cross-linker, and ADAM10 was detected by anti-HA Western blotting. The immature (*upper band*) and mature (*lower band*) forms of ADAM10 were detected and quantified using the Odyssey Infrared Imaging System from LI-COR Biosciences, and a graph is presented to show the mean total ADAM10 with S.E. from three experiments (**, $p < 0.01$ compared with all other tetraspanins). B, ADAM10 in whole cell lysates was similarly analyzed by anti-HA Western blotting, and a graph is presented to show the percentage of mature ADAM10 for each transfection ($n = 3$; **, $p < 0.01$ compared with ADAM10 only; *error bars* represent S.E.). C, expression of tetraspanins was confirmed by anti-FLAG Western blotting. The tetraspanins varied in their expression levels; Tspan2 was not readily detected in this figure but was detectable on longer exposures (data not shown). D–F, palmitoylation of Tspan14, Tspan15, and Tspan33 is not essential for ADAM10 interaction or promotion of maturation. The experiment was performed as described in A–C except that wild-type (WT) and palmitoylation mutant (PM) forms of human tetraspanins were compared, and the experiment was performed in 1% digitonin lysis buffer in the absence of DTSSP cross-linking (data are representative of three experiments; **, $p < 0.01$).

adopted using FLAG epitope-tagged tetraspanins and HA-tagged ADAM10. This was followed by surface chemical cross-linking with DTSSP with the aim of capturing direct tetraspanin-ADAM10 associations and co-immunoprecipitation under highly stringent lysis conditions (1% Triton, 0.1% SDS) to retain only cross-linked interactions. Importantly, DTSSP contains a disulfide bond that can be broken by reducing agents, thus allowing individual proteins to be detected by Western blotting at their appropriate molecular weights. This surface chemical cross-linking protocol has the added benefit of restricting the analysis to surface proteins, therefore avoiding intracellular aggregated proteins that can be a problem in transient transfection of HEK-293T cells. Following immunoprecipitation of the 10 tetraspanins, Tspan14, Tspan15, and Tspan33 shared the capacity to immunoprecipitate significantly more surface ADAM10 than the others (Fig. 2A). These three tetraspanins each interacted preferentially with the low molecular weight form of ADAM10, which corresponds to mature ADAM10 with a cleaved prodomain. In addition, Western blotting of whole cell lysates showed that Tspan14, Tspan15, and Tspan33 each promoted significant maturation of ADAM10 (Fig. 2B). Finally, expression of each tetraspanin was confirmed, albeit at levels that varied from relatively strong for CD9, Tspan14, Tspan15, and Tspan33 to relatively weak for Tspan2, which was only detectable upon longer exposures (Fig.

2C and data not shown). Taken together, these data suggest that among platelet tetraspanins Tspan14, Tspan15, and Tspan33 interact with ADAM10 and promote its maturation. This is the first reported function for Tspan14 or Tspan15; a gene knockout study has demonstrated an essential role for Tspan33 in mouse erythropoiesis (22).

Tetraspanin Palmitoylation Is Not Required for Tspan14, Tspan15, and Tspan33 to Promote ADAM10 Maturation—Palmitoylation of tetraspanins on multiple cysteine residues at their transmembrane-cytoplasmic junctions is known to promote tetraspanin-tetraspanin interaction and the formation of tetraspanin microdomains. Indeed, mutation of these cysteines impairs tetraspanin-tetraspanin interactions (12). If such mutants of Tspan14, Tspan15, and Tspan33 retained the capacity to regulate ADAM10, this would provide additional evidence in favor of a direct interaction (that is, an interaction that is not due to chemical cross-linking of a complex of proteins containing transfected proteins and endogenous tetraspanins that act as linkers). Interestingly, the previously reported regulation of ADAM10 by Tspan12 was dependent on palmitoylation of the latter (24), raising the possibility that the observed interaction was indirect. In an experiment with the same methodology as that shown previously in Fig. 2, A–C, palmitoylation mutants of Tspan14, Tspan15, and Tspan33 retained the capac-

TspanC8 Subgroup Regulates ADAM10 Maturation and Expression

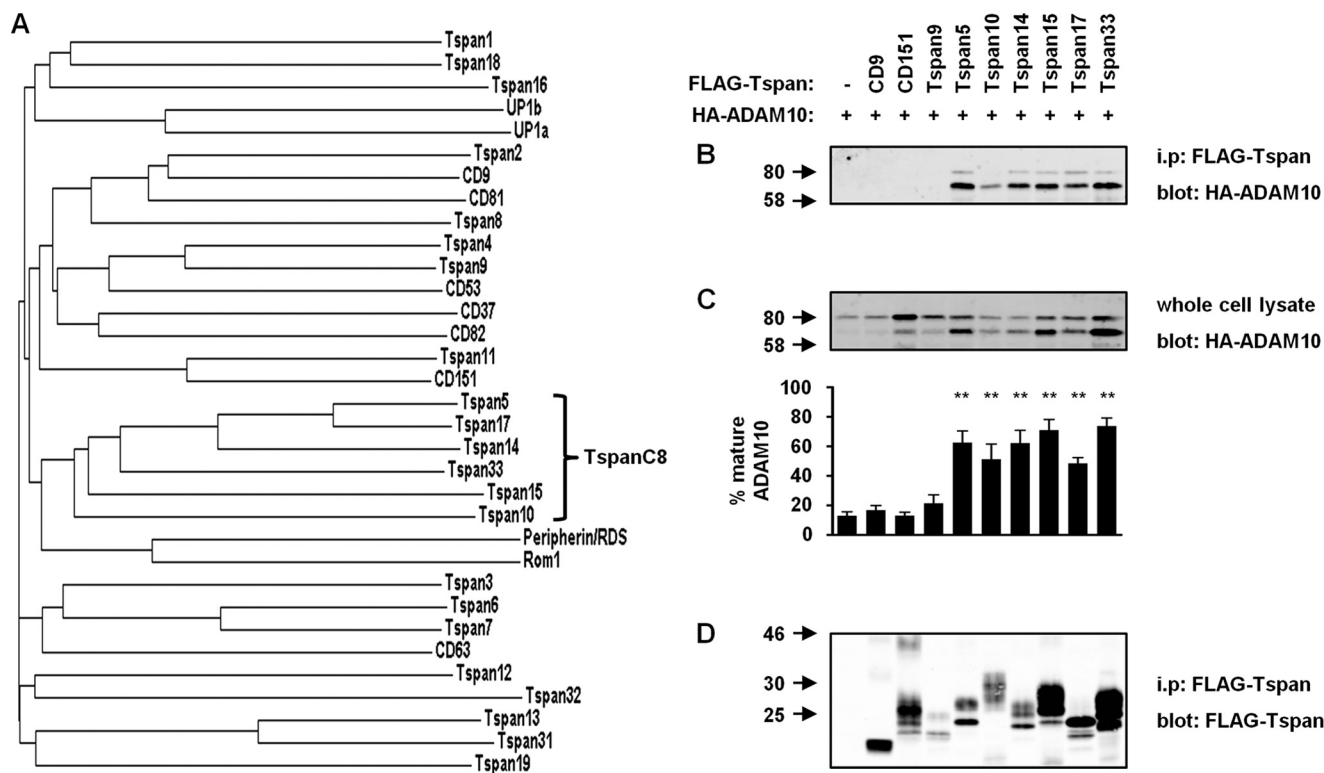


FIGURE 3. Tspan14, Tspan15, and Tspan33 are members of the TspanC8 subfamily of tetraspanins, which includes Tspan5, Tspan10, and Tspan17, and each can interact with and promote ADAM10 maturation. *A*, amino acid sequences of the 33 human tetraspanins were analyzed by the multiple sequence alignment tool Clustal Omega, which is a recently improved version of ClustalW (39), and the data are presented as a dendrogram. *B–D*, HEK-293T cells were transfected with HA-tagged bovine ADAM10 and FLAG-tagged forms of the six mouse TspanC8 and three non-TspanC8 tetraspanins. Cells were lysed in 1% digitonin and subjected to anti-FLAG immunoprecipitation (*i.p.*) followed by anti-HA and anti-FLAG Western blotting. Cells were lysed in 1% digitonin as described in Fig. 2, *A–C*. The data are representative of three experiments (**, $p < 0.01$; error bars represent S.E.).

ity to interact with surface ADAM10 and to promote its maturation (supplemental Fig. II).

To provide further evidence in support of these observations, co-immunoprecipitations were performed from non-cross-linked cells lysed in 1% digitonin. This is a detergent that precipitates cholesterol and large tetraspanin complexes but in which smaller tetraspanin-partner interactions appear to remain soluble (38). Indeed, digitonin has previously proved useful in identifying tetraspanin-partner interactions (12). Under digitonin lysis conditions, Tspan14, Tspan15, and Tspan33 co-immunoprecipitated robustly with ADAM10 in a manner that did not require palmitoylation of the tetraspanins (Fig. 2*D*). Promotion of ADAM10 maturation also did not require palmitoylation (Fig. 2*E*). As controls, mutation of palmitoylation sites did not affect tetraspanin expression (Fig. 2*F*), and CD9 failed to co-immunoprecipitate with ADAM10 or promote its maturation (Fig. 2, *D–F*). Taken together, these data are consistent with a direct interaction between ADAM10 and the tetraspanins Tspan14, Tspan15, and Tspan33.

Tspan14, Tspan15, and Tspan33 Are Members of the TspanC8 Subgroup of Tetraspanins—Tspan14, Tspan15, and Tspan33 share a relatively high protein sequence identity of between 31 and 39% in human and belong to a subgroup of six related tetraspanins that includes the functionally uncharacterized Tspan5, Tspan10, and Tspan17 (Fig. 3*A*). These six tetraspanins have eight cysteine residues within their main extracellular region unlike other tetraspanins that have four, six, or

seven. These cysteines appear to be structurally important through the formation of disulfide bonds (12). Hence, we have termed these six tetraspanins the TspanC8 subgroup.

To determine whether all six TspanC8 tetraspanins share the capacity to interact with and promote ADAM10 maturation, ADAM10 was co-transfected into HEK-293T cells with each TspanC8 tetraspanin, and ADAM10 co-immunoprecipitation and maturation following digitonin lysis were detected by Western blotting as described in Fig. 2, *D–F*. The TspanC8 tetraspanins each interacted with ADAM10, but control tetraspanins CD9, CD151, and Tspan9 did not (Fig. 3*B*). Among the TspanC8 tetraspanins, Tspan10 interacted with ADAM10 relatively poorly (Fig. 3*B*), which was consistently observed in three experiments (data not shown). Nevertheless, each TspanC8 tetraspanin promoted significant ADAM10 maturation unlike the non-TspanC8 tetraspanin controls (Fig. 3*C*), and expression of the tetraspanins was confirmed in Fig. 3*D*. These data suggest that the six TspanC8 tetraspanins share a common function in regulating ADAM10.

Tspan12 is not a TspanC8 tetraspanin (Fig. 3*A*) but was reported previously to promote ADAM10 maturation (24). However, this study did not include any TspanC8 tetraspanins that would have allowed their comparison with Tspan12. To address whether TspanC8 tetraspanins and Tspan12 interact with ADAM10 and promote maturation in a comparable manner, interaction and maturation were measured by co-immunoprecipitation in digitonin lysis buffer. In these experiments,

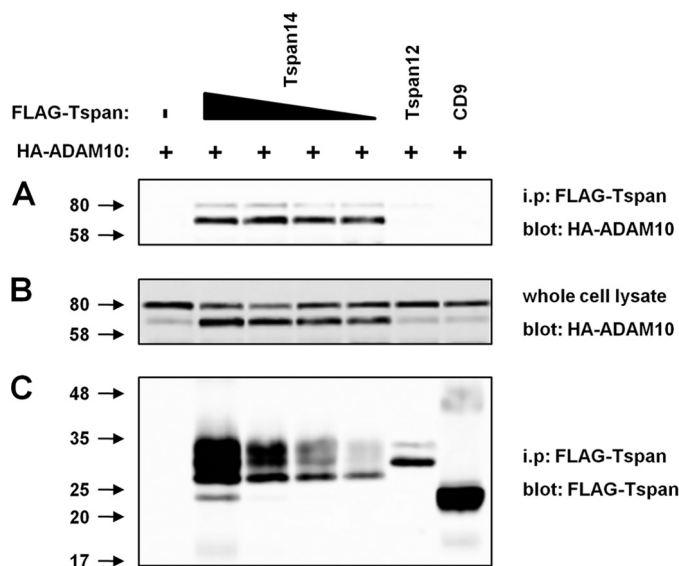


FIGURE 4. The non-TspanC8 tetraspanin Tspan12 does not interact with or promote ADAM10 maturation. HEK-293T cells were transfected with HA-tagged bovine ADAM10 and FLAG-tagged mouse forms of the non-TspanC8 tetraspanins Tspan12 or CD9 or a titration of the TspanC8 tetraspanin Tspan14. Cells were lysed in 1% digitonin and subjected to anti-FLAG immunoprecipitation (*i.p.*) followed by anti-HA Western blotting of immunoprecipitates (A) and whole cell lysates (B) and anti-FLAG blotting of immunoprecipitates (C).

the amount of transfected FLAG-Tspan14 was titrated down to allow comparison with the relatively poorly expressed FLAG-Tspan12. Unlike Tspan14, Tspan12 did not interact with ADAM10 (Fig. 4A) or induce ADAM10 maturation (Fig. 4B) despite similar expression levels at the lower end of the Tspan14 titration (Fig. 4C). In a complimentary set of experiments, GFP-tagged tetraspanins were used because GFP-Tspan12 was expressed at a level comparable with that of GFP-Tspan14, and the DTSSP cross-linking method was used as described previously in Fig. 2, A–C (supplemental Fig. III). Consistent with FLAG-Tspan12 in Fig. 4, GFP-Tspan12 failed to interact with ADAM10 or promote its maturation (supplemental Fig. III). Taken together with the previously published data, this suggests that although Tspan12 can induce ADAM10 maturation under some circumstances the TspanC8 tetraspanins may be the major tetraspanin regulators of ADAM10.

Tspan14 Is the Major TspanC8 Tetraspanin in HUVECs and Is Essential for Normal ADAM10 Surface Expression—Because overexpression of TspanC8 tetraspanins promotes ADAM10 maturation, a process that occurs during ADAM10 trafficking to the plasma membrane, it is possible that TspanC8 tetraspanins are required for such trafficking. This would be comparable with the way in which other tetraspanins are known to promote trafficking of other partners (12, 40). To test this theory, siRNA knockdown of TspanC8 tetraspanins was carried out followed by flow cytometry to detect surface ADAM10 expression. Because siRNA knockdown is not possible in platelets, primary HUVECs were selected because of the importance of ADAM10 in endothelial cell function (1). To initially determine the relative expression levels of TspanC8 tetraspanins in HUVECs, RT-PCR was carried out because effective antibodies are not available to any TspanC8 tetraspanin. Tspan14 mRNA was found to be more abundant than the rest of the TspanC8

tetraspanins combined (Fig. 5A). These data were comparable with next generation sequencing of HUVECs that yielded the following number of mRNA transcripts per million: 9.1 for Tspan5, 0.1 for Tspan10, 56.9 for Tspan14, 14.6 for Tspan15, 24.7 for Tspan17, and 0 for Tspan33.³ Tspan14 knockdown with two different siRNA duplexes was found to decrease Tspan14 mRNA by over 75% as detected by RT-PCR (Fig. 5B). More importantly, each significantly reduced surface ADAM10 by over 50% (Fig. 5, C and D). It is possible that residual Tspan14 and other TspanC8 tetraspanins in these cells is the reason why the reduction in surface ADAM10 was not complete.

To determine the effect of Tspan14 knockdown on ADAM10 activity, HUVEC lysates were Western blotted for the ADAM10 substrate VE-cadherin (10). Tspan14 knockdown significantly reduced VE-cadherin cleavage in line with the reduction in ADAM10 expression level (Fig. 5, E and F). As an additional control, VE-cadherin cleavage was further reduced by ADAM10 knockdown (Fig. 5, E and F), and the level of ADAM10 protein knockdown was almost 100% as detected by flow cytometry (Fig. 5C). In combination with the flow cytometry data, these ADAM10 activity data are consistent with the idea that TspanC8 tetraspanins are essential for normal ADAM10 surface expression.

ADAM10 Stability in the A549 Cell Line Is Not Reduced following Tspan14 Knockdown—The reduced ADAM10 surface expression following Tspan14 knockdown could be due to impaired trafficking to the cell surface and/or reduced stability. To address the latter possibility, a cell surface biotinylation assay was used in Tspan14 knockdown A549 human lung epithelial cells. This cell line was chosen for these experiments because its TspanC8 tetraspanin profile is similar to that of HUVECs (Fig. 6A). In addition, A549 has the advantage of being a faster growing cell line that is more amenable to biochemical analyses than primary HUVECs. Similar to HUVECs, Tspan14 knockdown significantly reduced the level of surface ADAM10, which in this case was detected by surface biotinylation and ADAM10 immunoprecipitation followed by neutravidin Western blotting (Fig. 6, B and C). However, there was no evidence for increased ADAM10 degradation following Tspan14 knockdown relative to negative control siRNA over 24, 36, and 48 h postbiotinylation (Fig. 6B). Instead, quantitation revealed that loss of biotinylated ADAM10 over time appeared slightly slower following Tspan14 knockdown (Fig. 6C). These data suggest that impaired ADAM10 trafficking to the cell surface is the main consequence of Tspan14 knockdown.

Tspan33 Is the Major TspanC8 Tetraspanin in the Erythrocyte Lineage and Is Essential for Normal ADAM10 Expression—To determine whether TspanC8 tetraspanins regulate ADAM10 *in vivo*, ADAM10 expression was investigated in cells from the Tspan33-deficient mouse, which is the only currently available knock-out mouse for a TspanC8 tetraspanin (22). The two major blood cell types, platelets and erythrocytes, were selected as the subjects of this analysis because their relative Tspan33 expression levels were likely to be quite distinct; Tspan33 mRNA is expressed by mouse erythrocytes (22) but is

³ J. M. Herbert and R. Bicknell, unpublished data.

TspanC8 Subgroup Regulates ADAM10 Maturation and Expression

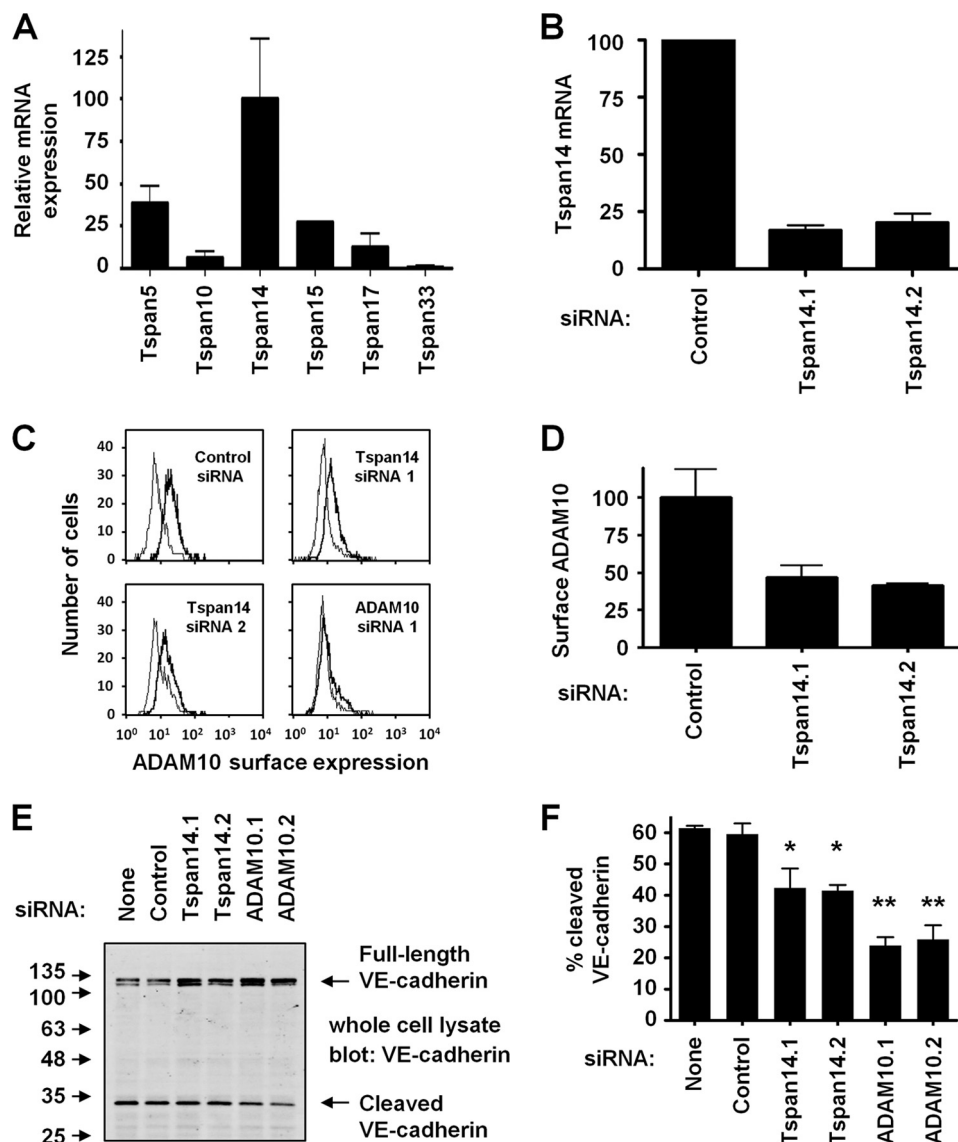


FIGURE 5. Surface ADAM10 expression is reduced upon knockdown of the major HUVEC TspanC8 tetraspanin Tspan14. *A*, the mRNA levels of TspanC8 tetraspanins in HUVECs were measured by RT-PCR ($n = 2$; error bars represent S.E.). *B*, HUVECs were transfected with negative control siRNA or two different Tspan14 siRNAs. Tspan14 knockdown was assessed by RT-PCR ($n = 2$; error bars represent S.E.). *C*, HUVEC surface ADAM10 levels were measured by flow cytometry in the transfected cells from *B*. Representative histograms include an ADAM10 knockdown as a control. For each histogram, the ADAM10 trace is in black, and the isotype antibody control is in gray. *D*, the data in *C* are also presented as a bar chart showing mean ADAM10 levels and S.E. from two experiments. *E* and *F*, HUVECs were transfected with negative control siRNA or two different Tspan14 or ADAM10 siRNAs. Whole cell lysates were subjected to Western blotting for the cytoplasmic tail of the ADAM10 substrate VE-cadherin (*E*). A graph shows the mean percentage of cleaved ADAM10 with S.E. from three experiments (*F*) (*, $p < 0.05$; **, $p < 0.01$ compared with the non-transfected control).

minimal in mouse platelets (supplemental Fig. 1). To test this hypothesis, TspanC8 tetraspanin mRNA levels were measured by RT-PCR in mouse megakaryocytes and erythroid progenitors because mature platelets and erythrocytes carry relatively small amounts of mRNA. Tspan33 expression in mouse megakaryocytes was almost undetectable in contrast to the relatively high expression of Tspan14 and weaker expression of Tspan5 and Tspan17 (Fig. 7A). Conversely, Tspan33 was the major TspanC8 tetraspanin in erythroid progenitors compared with almost undetectable levels of Tspan5 and Tspan14 (Fig. 7B). No compensatory up-regulation of other TspanC8 tetraspanins was apparent in Tspan33-deficient cells (data not shown). As a control, primer/probe efficiencies were found to be similar for each TspanC8 tetraspanin (supplemental Fig. 4V).

Consistent with the extremely low relative level of Tspan33 in megakaryocytes, ADAM10 surface expression was normal on Tspan33-deficient mouse platelets (Fig. 7C). In contrast, Tspan33-deficient erythrocytes exhibited an approximate 90% reduction in surface ADAM10 (Fig. 7D), which was consistent with similarly reduced whole cell ADAM10 expression as determined by Western blotting (Fig. 7E). Importantly, defective ADAM10 protein expression was not due to any reduction in ADAM10 mRNA in the erythroid lineage (Fig. 7F). Together these data demonstrate that TspanC8 tetraspanins regulate ADAM10 *in vivo*. The distinct repertoires of TspanC8 tetraspanins in different cell types may allow ADAM10 targeting to specific substrates and may ultimately be exploited in therapies that target specific TspanC8-ADAM10 complexes.

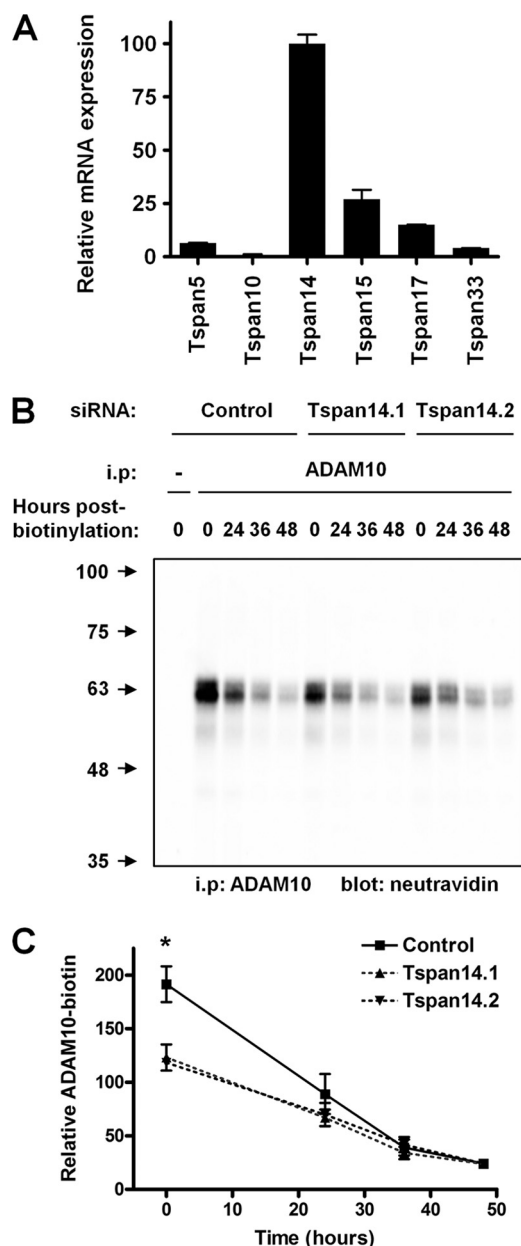


FIGURE 6. Tspan14 knockdown in the A549 epithelial cell line does not reduce ADAM10 stability. *A*, the mRNA levels of TspanC8 tetraspanins in A549 cells were measured by RT-PCR ($n = 2$; error bars represent S.E.). *B*, A549 cells were transfected with negative control siRNA or two different siRNAs to Tspan14, the major TspanC8 tetraspanin in this cell type. Cells were surface-biotinylated and lysed at 0, 24, 36, and 48 h postbiotinylation. Lysates were subjected to immunoprecipitation (*i.p.*) with ADAM10 or negative control mAbs and then Western blotted with neutravidin to detect biotinylated ADAM10, the size of which corresponds to the mature form. The blot shown is representative of three experiments. *C*, ADAM10 levels from *B* and two additional experiments were quantified using the Odyssey Infrared Imaging System, and a graph is presented to show the mean level of biotinylated ADAM10 with S.E. ($n = 3$; *, $p < 0.05$ for control siRNA versus Tspan14 siRNA knockdowns).

DISCUSSION

The metalloprotease ADAM10 cleaves over 40 transmembrane targets, including the platelet-activating collagen receptor glycoprotein VI (7, 8). Because ADAM10 is compartmentalized into tetraspanin membranes on various cell types (23, 24), including platelets (Fig. 1), the present study began with the

hypothesis that one or more platelet tetraspanins would specifically associate with and regulate ADAM10. This hypothesis was proved correct by the discovery that three platelet tetraspanins could interact with and promote ADAM10 maturation. These were Tspan14, Tspan15, and Tspan33, the former two of which were previously uncharacterized. Because of their relatively strong sequence identities, including eight cysteine residues within their major extracellular region, they were named the TspanC8 subgroup of tetraspanins. This subgroup contains three other uncharacterized tetraspanins, Tspan5, Tspan10, and Tspan17, which each were able to interact with and promote ADAM10 maturation. Furthermore, analyses of the only available knock-out mouse for a TspanC8 tetraspanin (Tspan33) and tetraspanin knockdown in cultured primary endothelial cells demonstrated an essential role for TspanC8 tetraspanins in ADAM10 trafficking to the cell surface. Reduced endothelial cell surface ADAM10 correlated with reduced activity toward its substrate (VE-cadherin). This study has therefore defined a function for a largely uncharacterized subgroup of tetraspanins and has identified a novel global regulatory mechanism for ADAM10.

The hypothesis behind this work was conceived following two previous reports that ADAM10 was tetraspanin-associated in leukocyte, breast cancer, and neuroblastoma cell lines (23, 24). Moreover, Tspan12 was proposed as an ADAM10-interacting tetraspanin (24). However, because ADAM10 appears to be ubiquitous but Tspan12 is not (16), it seemed likely that other tetraspanins would interact with ADAM10. Analyses of the Tspan12-deficient mouse did not address a potential role in ADAM10 regulation but instead demonstrated a role for Tspan12 in the regulation of Frizzled-4-induced β -catenin signaling (16). Tspan12 deficiency leads to defective vascular development in the retina, and Tspan12 mutations cause the human blinding disease familial exudative vitreoretinopathy, thus phenocopying mutations in the Frizzled-4 signaling pathway (17, 18). To address whether Tspan12 could regulate ADAM10 in a manner comparable with that of TspanC8 tetraspanins, Tspan12 was compared with Tspan14 for its capacity to interact with and promote ADAM10 maturation. Using two different transiently transfected Tspan12 constructs (FLAG- and GFP-tagged) in two different types of co-immunoprecipitation experiment (digitonin lysis or DTSSP surface cross-linking), Tspan12 appeared unable to interact with ADAM10 and promote its maturation. How can this finding be resolved with the previous, apparently contradictory publication (24)? It is possible that this earlier finding was a consequence of up-regulation of TspanC8 expression at the transcriptional level due to the stable Tspan12 transfection used in the study (24). Tspan12 transfection can certainly promote Frizzled-4-induced β -catenin signaling in a cell line model (16), and this could in theory induce the transcription of one or more TspanC8 tetraspanins. This could facilitate indirect Tspan12 interaction with ADAM10 and maturation of the latter (24). A candidate is Tspan5, which was identified as a β -catenin target gene in a microarray screen of colorectal cancer cells (41). Consistent with the theory that the previously observed Tspan12-ADAM10 interaction could be bridged by a TspanC8 tetraspanin, the interaction was only detected in relatively non-stringent lysis

TspanC8 Subgroup Regulates ADAM10 Maturation and Expression

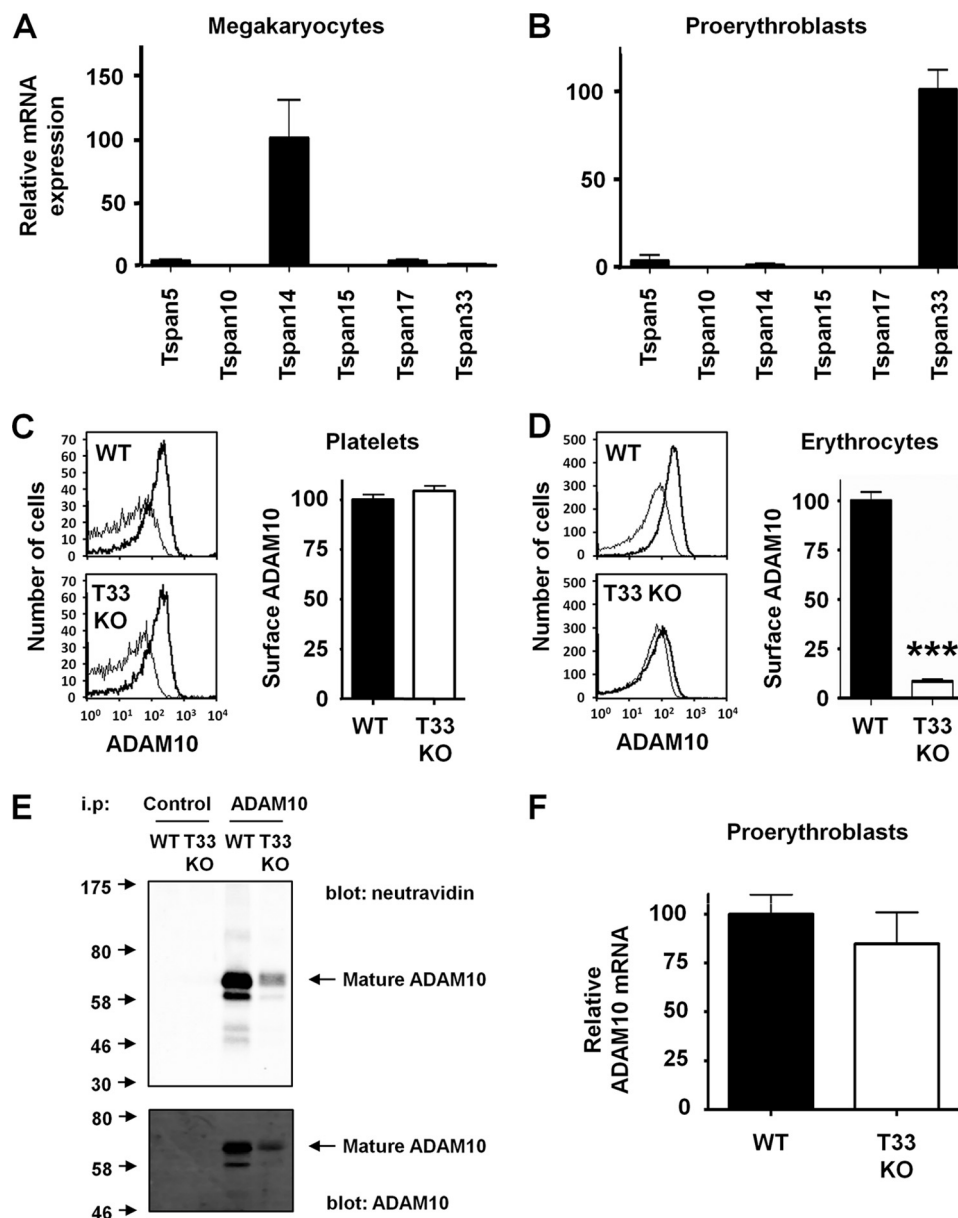


FIGURE 7. Regulation of ADAM10 expression by TspanC8 tetraspanins in the platelet and erythrocyte lineages. *A*, Tspan33 is relatively weakly expressed in the megakaryocyte/platelet lineage. The mRNA levels of TspanC8 tetraspanins in megakaryocytes isolated from wild-type mice were measured by RT-PCR ($n = 4$; error bars represent the S.E.). *B*, Tspan33 is relatively highly expressed in the erythroid lineage. The mRNA levels of TspanC8 tetraspanins in proerythroblasts isolated from wild-type mice were measured by RT-PCR ($n = 3$; error bars represent the S.E.). *C*, ADAM10 surface protein expression is normal on Tspan33-deficient platelets. Whole blood from WT and Tspan33 knock-out (*T33 KO*) mice was analyzed by flow cytometry for ADAM10, and platelets were gated by size. Representative histograms show the ADAM10 trace in black and the isotype control antibody in gray. The mean ADAM10 expression from five experiments is also presented as a bar chart (error bars represent the S.E.). *D*, erythrocyte surface ADAM10 expression is reduced by ~90% in the absence of Tspan33. Whole blood from WT and Tspan33 knock-out (*T33 KO*) mice was analyzed by flow cytometry for ADAM10, and erythrocytes were gated by size with the data presented as in *C* ($n = 5$; ***, $p < 0.001$; error bars represent the S.E.). *E*, whole cell ADAM10 expression is reduced in the absence of Tspan33. Erythrocytes from WT and Tspan33 knock-out (*T33 KO*) mice were surface-biotinylated, lysed in 1% Brij97 lysis buffer, and subjected to immunoprecipitation (*i.p.*) with isotype control or anti-ADAM10 antibody. The immunoprecipitates were Western blotted with neutravidin to detect biotinylated proteins (*upper panel*) or ADAM10 antibody (*lower panel*), the latter of which corresponded to the molecular weight of mature ADAM10. *F*, ADAM10 mRNA expression is normal in Tspan33-deficient erythroid progenitors. ADAM10 mRNA levels in proerythroblasts from WT and Tspan33 knock-out (*T33 KO*) mice were measured by RT-PCR ($n = 3$; error bars represent the S.E.).

conditions (0.5% Brij97) (24) that would maintain tetraspanin-tetraspanin interactions (12). Indeed, the interaction and ADAM10 maturation were lost upon mutation of the Tspan12 palmitoylation sites (24), which are required for normal tetraspanin-tetraspanin association (12). Importantly, mutation of palmitoylation sites in the TspanC8 tetraspanins did not abolish maturation of ADAM10 or significantly inhibit the

interaction in the present study, suggesting that these are *bona fide* ADAM10-interacting tetraspanins.

The key finding that TspanC8 tetraspanin deficiency results in reduced ADAM10 cell surface expression could potentially be due to impaired trafficking to the plasma membrane and/or reduced ADAM10 stability. Reduced stability is unlikely to be involved because knockdown of Tspan14, the major TspanC8

tetraspanin in the A549 epithelial cell line, failed to show any increased ADAM10 degradation over time using a cell surface biotinylation approach. Importantly, ADAM10 surface expression was significantly reduced by Tspan14 knockdown at the beginning of the experiment. Therefore, TspanC8 tetraspanins are likely to promote ADAM10 trafficking to the cell surface. Promotion of partner trafficking is emerging as a general concept in tetraspanin biology. For example, tetraspanin CD81 is essential for normal surface trafficking of CD19, a key component of B cell receptor signaling, such that mutation of CD81 in humans results in a loss of surface CD19 and profound immunodeficiency (40). An important question that arises from the current study concerns the mechanism by which the TspanC8 tetraspanins promote trafficking of ADAM10 to the cell surface. ADAM10 was recently shown to possess an arginine-based endoplasmic reticulum (ER) retention motif that prevents efficient trafficking of the metalloprotease to the cell surface (42). However, it was not clear from that study how the retention motif is overcome and ADAM10 is released from the ER. One theory in the study of such arginine-based ER retention motifs is that they can be masked upon successful interaction with a partner protein, which then allows the correctly assembled complex to be transported from the ER (43). It is therefore possible that ADAM10 is retained in the ER until interaction with a TspanC8 tetraspanin, which masks the retention motif.

A striking finding from the present study was that as many as six tetraspanins could regulate ADAM10. Such functional compensation among tetraspanins is not without precedent albeit on a smaller scale. The clearest example is for the related tetraspanins CD9 and CD81, which share 44% protein sequence identity in human and share some common partners, namely the immunoglobulin superfamily proteins EWI-2 and EWI-F (CD9P-1) (12). CD81 was shown to partially compensate for the fertilization defect observed in CD9-deficient mice (12). In addition, a role for these tetraspanins in the maintenance of normal lung function was only revealed by the observation of a chronic obstructive pulmonary disease-like phenotype in the double knock-out mouse but not in either of the single knock-outs (44). Compensation between TspanC8 tetraspanins is likely to complicate future analyses of knockdown cells and knock-out animals. An additional problem is the lack of effective antibodies to any TspanC8 tetraspanin, which leaves RT-PCR as the current best option for quantifying mRNA expression levels in different cell types. This technique was used in the present study to demonstrate that Tspan33 and Tspan14 are the major TspanC8 tetraspanins in mouse erythroid cells and HUVECs, respectively. This explains the striking reductions in surface ADAM10 on erythrocytes and HUVECs deficient for these tetraspanins. The Tspan33-deficient mice used in this study exhibit impaired erythropoiesis (22), but it is currently unclear whether an ~90% reduction in surface ADAM10 could be responsible for this phenotype. Finally, ADAM10 was found to be normally expressed on the surface of platelets from these mice, which was consistent with the almost undetectable level of Tspan33 mRNA in their megakaryocyte precursors. Because Tspan14 is the major TspanC8 tetraspanin in this lineage, defective platelet ADAM10 expression in a Tspan14 knock-out mouse would be predicted.

ADAM10 has considerable therapeutic potential due to the important roles of its many target proteins in inflammation, thrombosis, cancer, and Alzheimer disease (1, 4). Despite its potential in therapy, all clinical trials involving ADAM10 have so far failed due to problems with toxicity (4). However, this study has identified the TspanC8 tetraspanins as the regulators of ADAM10 maturation and trafficking to the cell surface. The ADAM10 interaction with six TspanC8 tetraspanins may have evolved to allow targeting of ADAM10 to specific substrates or compartments within the cell. Targeting specific TspanC8 tetraspanin-ADAM10 complexes raises the possibility of targeting the metalloprotease in a cell type- or substrate-specific manner. Such an approach could target specific disease processes such as cancer, Alzheimer disease, and cardiovascular disease while minimizing problems with toxicity.

Acknowledgments—We thank Eric Rubinstein for reagents and discussions, Victoria Heath for comments on the manuscript, Alexandra Mazharian for megakaryocyte advice, the Biomedical Services Unit for housing mice, and Phil Stone for providing HUVECs. We are also grateful to John Herbert and Roy Bicknell for sharing unpublished data.

Addendum—Prox *et al.* (45) have recently identified the TspanC8 tetraspanin Tspan15 in a screen for ADAM10-interacting proteins. Consistent with our data on Tspan14, Tspan33, and other TspanC8 tetraspanins, Tspan15 was found to promote ADAM10 exit from the endoplasmic reticulum, maturation, cell surface expression, and activity (45).

REFERENCES

1. Drey Mueller, D., Pruessmeyer, J., Groth, E., and Ludwig, A. (2012) The role of ADAM-mediated shedding in vascular biology. *Eur. J. Cell Biol.* **91**, 472–485
2. Glomski, K., Monette, S., Manova, K., De Strooper, B., Saftig, P., and Blobel, C. P. (2011) Deletion of Adam10 in endothelial cells leads to defects in organ-specific vascular structures. *Blood* **118**, 1163–1174
3. Zhang, C., Tian, L., Chi, C., Wu, X., Yang, X., Han, M., Xu, T., Zhuang, Y., and Deng, K. (2010) Adam10 is essential for early embryonic cardiovascular development. *Dev. Dyn.* **239**, 2594–2602
4. Saftig, P., and Reiss, K. (2011) The “A Disintegrin And Metalloproteases” ADAM10 and ADAM17: novel drug targets with therapeutic potential? *Eur. J. Cell Biol.* **90**, 527–535
5. Hartmann, D., de Strooper, B., Serneels, L., Craessaerts, K., Herreman, A., Annaert, W., Umans, L., Lübke, T., Lena Illert, A., von Figura, K., and Saftig, P. (2002) The disintegrin/metalloprotease ADAM 10 is essential for Notch signalling but not for α -secretase activity in fibroblasts. *Hum. Mol. Genet.* **11**, 2615–2624
6. Postina, R., Schroeder, A., Dewachter, I., Bohl, J., Schmitt, U., Kojro, E., Prinsen, C., Endres, K., Hiemke, C., Blessing, M., Flamez, P., Dequenne, A., Godaux, E., van Leuven, F., and Fahrenholz, F. (2004) A disintegrin-metalloproteinase prevents amyloid plaque formation and hippocampal defects in an Alzheimer disease mouse model. *J. Clin. Investig.* **113**, 1456–1464
7. Bender, M., Hofmann, S., Stegner, D., Chalaris, A., Bösl, M., Braun, A., Scheller, J., Rose-John, S., and Nieswandt, B. (2010) Differentially regulated GPVI ectodomain shedding by multiple platelet-expressed proteinases. *Blood* **116**, 3347–3355
8. Gardiner, E. E., Karunakaran, D., Shen, Y., Arthur, J. F., Andrews, R. K., and Berndt, M. C. (2007) Controlled shedding of platelet glycoprotein (GP)VI and GPIb-IX-V by ADAM family metalloproteinases. *J. Thromb. Haemost.* **5**, 1530–1537
9. Donners, M. M., Wolfs, I. M., Olieslagers, S., Mohammadi-Motahhari, Z.,

TspanC8 Subgroup Regulates ADAM10 Maturation and Expression

- Tchaikovski, V., Heeneman, S., van Buul, J. D., Caolo, V., Molin, D. G., Post, M. J., and Waltenberger, J. (2010) A disintegrin and metalloprotease 10 is a novel mediator of vascular endothelial growth factor-induced endothelial cell function in angiogenesis and is associated with atherosclerosis. *Arterioscler. Thromb. Vasc. Biol.* **30**, 2188–2195
10. Schulz, B., Pruessmeyer, J., Maretzky, T., Ludwig, A., Blobel, C. P., Saftig, P., and Reiss, K. (2008) ADAM10 regulates endothelial permeability and T-Cell transmigration by proteolysis of vascular endothelial cadherin. *Circ. Res.* **102**, 1192–1201
11. Hundhausen, C., Schulte, A., Schulz, B., Andrzejewski, M. G., Schwarz, N., von Hundelshausen, P., Winter, U., Paliga, K., Reiss, K., Saftig, P., Weber, C., and Ludwig, A. (2007) Regulated shedding of transmembrane chemokines by the disintegrin and metalloproteinase 10 facilitates detachment of adherent leukocytes. *J. Immunol.* **178**, 8064–8072
12. Charrin, S., le Naour, F., Silvie, O., Milhiet, P. E., Boucheix, C., and Rubinstein, E. (2009) Lateral organization of membrane proteins: tetraspanins spin their web. *Biochem. J.* **420**, 133–154
13. Yáñez-Mó, M., Barreiro, O., Gordon-Alonso, M., Sala-Valdés, M., and Sánchez-Madrid, F. (2009) Tetraspanin-enriched microdomains: a functional unit in cell plasma membranes. *Trends Cell Biol.* **19**, 434–446
14. Barreiro, O., Zamai, M., Yáñez-Mó, M., Tejera, E., López-Romero, P., Monk, P. N., Gratton, E., Caiola, V. R., and Sánchez-Madrid, F. (2008) Endothelial adhesion receptors are recruited to adherent leukocytes by inclusion in preformed tetraspanin nanoplateforms. *J. Cell Biol.* **183**, 527–542
15. Doyle, E. L., Ridger, V., Ferraro, F., Turmaine, M., Saftig, P., and Cutler, D. F. (2011) CD63 is an essential cofactor to leukocyte recruitment by endothelial P-selectin. *Blood* **118**, 4265–4273
16. Junge, H. J., Yang, S., Burton, J. B., Paes, K., Shu, X., French, D. M., Costa, M., Rice, D. S., and Ye, W. (2009) TSPAN12 regulates retinal vascular development by promoting Norrin- but not Wnt-induced FZD4/ β -catenin signaling. *Cell* **139**, 299–311
17. Nikopoulos, K., Gilissen, C., Hoischen, A., van Nouhuys, C. E., Boonstra, F. N., Blokland, E. A., Arts, P., Wieskamp, N., Strom, T. M., Ayuso, C., Tilanus, M. A., Bouwhuis, S., Mukhopadhyay, A., Scheffer, H., Hoefsloot, L. H., Veltman, J. A., Cremers, F. P., and Collin, R. W. (2010) Next-generation sequencing of a 40 Mb linkage interval reveals TSPAN12 mutations in patients with familial exudative vitreoretinopathy. *Am. J. Hum. Genet.* **86**, 240–247
18. Poulter, J. A., Ali, M., Gilmour, D. F., Rice, A., Kondo, H., Hayashi, K., Mackey, D. A., Kearns, L. S., Ruddle, J. B., Craig, J. E., Pierce, E. A., Downey, L. M., Mohamed, M. D., Markham, A. F., Inglehearn, C. F., and Toomes, C. (2010) Mutations in TSPAN12 cause autosomal-dominant familial exudative vitreoretinopathy. *Am. J. Hum. Genet.* **86**, 248–253
19. Takeda, Y., Kazarov, A. R., Butterfield, C. E., Hopkins, B. D., Benjamin, L. E., Kaipainen, A., and Hemler, M. E. (2007) Deletion of tetraspanin Cd151 results in decreased pathologic angiogenesis *in vivo* and *in vitro*. *Blood* **109**, 1524–1532
20. Goschnick, M. W., Lau, L. M., Wee, J. L., Liu, Y. S., Hogarth, P. M., Robb, L. M., Hickey, M. J., Wright, M. D., and Jackson, D. E. (2006) Impaired “outside-in” integrin α IIb β 3 signaling and thrombus stability in TSSC6-deficient mice. *Blood* **108**, 1911–1918
21. Orłowski, E., Chand, R., Yip, J., Wong, C., Goschnick, M. W., Wright, M. D., Ashman, L. K., and Jackson, D. E. (2009) A platelet tetraspanin superfamily member, CD151, is required for regulation of thrombus growth and stability *in vivo*. *J. Thromb. Haemost.* **7**, 2074–2084
22. Heikens, M. J., Cao, T. M., Morita, C., Dehart, S. L., and Tsai, S. (2007) Penumbra encodes a novel tetraspanin that is highly expressed in erythroid progenitors and promotes effective erythropoiesis. *Blood* **109**, 3244–3252
23. Arduise, C., Abache, T., Li, L., Billard, M., Chabanon, A., Ludwig, A., Mauduit, P., Boucheix, C., Rubinstein, E., and Le Naour, F. (2008) Tetraspanins regulate ADAM10-mediated cleavage of TNF- α and epidermal growth factor. *J. Immunol.* **181**, 7002–7013
24. Xu, D., Sharma, C., and Hemler, M. E. (2009) Tetraspanin12 regulates ADAM10-dependent cleavage of amyloid precursor protein. *FASEB J.* **23**, 3674–3681
25. Haining, E. J., Yang, J., and Tomlinson, M. G. (2011) Tetraspanin microdomains: fine-tuning platelet function. *Biochem. Soc. Trans.* **39**, 518–523
26. Lewandrowski, U., Wortelkamp, S., Lohrig, K., Zahedi, R. P., Wolters, D. A., Walter, U., and Sickmann, A. (2009) Platelet membrane proteomics: a novel repository for functional research. *Blood* **114**, e10–e19
27. Protty, M. B., Watkins, N. A., Colombo, D., Thomas, S. G., Heath, V. L., Herbert, J. M., Bicknell, R., Senis, Y. A., Ashman, L. K., Berditchevski, F., Ouwehand, W. H., Watson, S. P., and Tomlinson, M. G. (2009) Identification of Tspan9 as a novel platelet tetraspanin and the collagen receptor GPVI as a component of tetraspanin microdomains. *Biochem. J.* **417**, 391–400
28. Rowley, J. W., Oler, A. J., Tolley, N. D., Hunter, B. N., Low, E. N., Nix, D. A., Yost, C. C., Zimmerman, G. A., and Weyrich, A. S. (2011) Genome-wide RNA-seq analysis of human and mouse platelet transcriptomes. *Blood* **118**, e101–111
29. Tomlinson, M. G. (2009) Platelet tetraspanins: small but interesting. *J. Thromb. Haemost.* **7**, 2070–2073
30. Sincock, P. M., Mayrhofer, G., and Ashman, L. K. (1997) Localization of the transmembrane 4 superfamily (TM4SF) member PETA-3 (CD151) in normal human tissues: comparison with CD9, CD63, and α 5 β 1 integrin. *J. Histochem. Cytochem.* **45**, 515–525
31. Tomlinson, M. G., Woods, D. B., McMahon, M., Wahl, M. I., Witte, O. N., Kurosaki, T., Bolen, J. B., and Johnston, J. A. (2001) A conditional form of Bruton’s tyrosine kinase is sufficient to activate multiple downstream signaling pathways via PLC γ 2 in B cells. *BMC Immunol.* **2**, 4
32. Lammich, S., Kojro, E., Postina, R., Gilbert, S., Pfeiffer, R., Jasionowski, M., Haass, C., and Jahn, H. (1999) Constitutive and regulated α -secretase cleavage of Alzheimer’s amyloid precursor protein by a disintegrin metalloprotease. *Proc. Natl. Acad. Sci. U.S.A.* **96**, 3922–3927
33. Ehrhardt, C., Schmolke, M., Matzke, A., Knoblauch, A., Will, C., Wixler, V., and Ludwig, S. (2006) Polyethylenimine, a cost-effective transfection reagent. *Signal Transduction* **6**, 179–184
34. Maciag, T., Cerundolo, J., Illesly, S., Kelley, P. R., and Forand, R. (1979) An endothelial cell growth factor from bovine hypothalamus: identification and partial characterization. *Proc. Natl. Acad. Sci. U.S.A.* **76**, 5674–5678
35. McCarty, O. J., Calaminus, S. D., Berndt, M. C., Machesky, L. M., and Watson, S. P. (2006) von Willebrand factor mediates platelet spreading through glycoprotein Ib and α (IIb) β 3 in the presence of botrocetin and ristocetin, respectively. *J. Thromb. Haemost.* **4**, 1367–1378
36. Dumon, S., Heath, V. L., Tomlinson, M. G., Göttgens, B., and Frampton, J. (2006) Differentiation of murine committed megakaryocytic progenitors isolated by a novel strategy reveals the complexity of GATA and Ets factor involvement in megakaryocytopoiesis and an unexpected potential role for GATA-6. *Exp. Hematol.* **34**, 654–663
37. Vegiopoulos, A., García, P., Emambokus, N., and Frampton, J. (2006) Co-ordination of erythropoiesis by the transcription factor c-Myb. *Blood* **107**, 4703–4710
38. Charrin, S., Manié, S., Thiele, C., Billard, M., Gerlier, D., Boucheix, C., and Rubinstein, E. (2003) A physical and functional link between cholesterol and tetraspanins. *Eur. J. Immunol.* **33**, 2479–2489
39. Sievers, F., Wilm, A., Dineen, D., Gibson, T. J., Karplus, K., Li, W., Lopez, R., McWilliam, H., Rimmert, M., Söding, J., Thompson, J. D., and Higgins, D. G. (2011) Fast, scalable generation of high-quality protein multiple sequence alignments using Clustal Omega. *Mol. Syst. Biol.* **7**, 539
40. van Zelm, M. C., Smet, J., Adams, B., Mascart, F., Schandené, L., Janssen, F., Ferster, A., Kuo, C. C., Levy, S., van Dongen, J. J., and van der Burg, M. (2010) CD81 gene defect in humans disrupts CD19 complex formation and leads to antibody deficiency. *J. Clin. Invest.* **120**, 1265–1274
41. van de Wetering, M., Sancho, E., Verweij, C., de Lau, W., Oving, I., Hurlstone, A., van der Horn, K., Batlle, E., Coudreuse, D., Haramis, A. P., Tjon-Pon-Fong, M., Moerer, P., van den Born, M., Soete, G., Pals, S., Eilers, M., Medema, R., and Clevers, H. (2002) The β -catenin/TCF-4 complex imposes a crypt progenitor phenotype on colorectal cancer cells. *Cell* **111**, 241–250
42. Marcello, E., Gardoni, F., Di Luca, M., and Pérez-Otaño, I. (2010) An arginine stretch limits ADAM10 exit from the endoplasmic reticulum. *J. Biol. Chem.* **285**, 10376–10384
43. Michelsen, K., Yuan, H., and Schwappach, B. (2005) Hide and run. Arginine-based endoplasmic-reticulum-sorting motifs in the assembly of het-

- eromultimeric membrane proteins. *EMBO Rep.* **6**, 717–722
44. Takeda, Y., He, P., Tachibana, I., Zhou, B., Miyado, K., Kaneko, H., Suzuki, M., Minami, S., Iwasaki, T., Goya, S., Kijima, T., Kumagai, T., Yoshida, M., Osaki, T., Komori, T., Mekada, E., and Kawase, I. (2008) Double deficiency of tetraspanins CD9 and CD81 alters cell motility and protease production of macrophages and causes chronic obstructive pulmonary disease-like phenotype in mice. *J. Biol. Chem.* **283**, 26089–26097
45. Prox, J., Willenbrock, M., Weber, S., Lehmann, T., Schmidt-Arras, D., Schwanbeck, R., Saftig, P., and Schwake, M. (2012) Tetraspanin15 regulates cellular trafficking and activity of the ectodomain sheddase ADAM10. *Cell. Mol. Life Sci.* **69**, 2919–2932